Bioresource Technology 140 (2013) 406–413

Contents lists available at SciVerse ScienceDirect

Bioresource Technology

journal homepage: www.elsevier.com/locate/biortech

Biochars prepared from anaerobic digestion residue, palm bark, and eucalyptus for adsorption of cationic methylene blue dye: Characterization, equilibrium, and kinetic studies

Lei Sun [a,b], Shungang Wan [a], Wensui Luo [a,*]

[a] Institute of Urban Environment, Chinese Academy of Sciences, Xiamen 361021, PR China
[b] School of Environment, Guangxi University, Nanning 530004, PR China

HIGHLIGHTS

- Biochars were produced from municipal organic solid waste through pyrolysis.
- Biochars were used for the removal of methylene blue dye (MB) – an hazardous pollutant.
- Biochar prepared from biogas residue has the highest adsorption efficiency.
- Adsorption behaviors was well described by pseudo-second-order kinetic model.
- Adsorption fitted well with Langmuir isotherms, suggesting monolayer adsorption.

ARTICLE INFO

Article history:
Received 9 March 2013
Received in revised form 28 April 2013
Accepted 29 April 2013
Available online 9 May 2013

Keywords:
Biochar
Anaerobic digestion residue
Palm bark
Eucalyptus
Adsorption

ABSTRACT

Biochars prepared from anaerobic digestion residue (BC-R), palm bark (BC-PB) and eucalyptus (BC-E) were used as sorbents for removal of cationic methylene blue dye (MB). The FE-SEM images indicated that the biochars have a well-developed pore structure, and the Brunauer–Emmett–Teller surface areas of BC-R, BC-PB, and BC-E were 7.60, 2.46, and 10.35 $m^2 g^{-1}$, respectively. The efficiencies of MB removal in the samples with initial concentrations of 5 $mg L^{-1}$ at pH 7.0 and 40 °C by BC-R, BC-PB, and BC-E after 2 h were 99.5%, 99.3%, and 86.1%, respectively. Pseudo-second-order kinetics was the most suitable model for describing the adsorption of MB onto the biochars. The experimental data were best described by the Langmuir isotherm model, with a maximum monolayer adsorption capacity of 9.50 $mg g^{-1}$ at 40 °C for BC-R. The biochars produced from the three types of solid waste showed considerable potential for adsorption.

© 2013 Elsevier Ltd. All rights reserved.

1. Introduction

The textile-dyeing industry consumes large quantities of water and produces large volumes of wastewater from different steps in the dyeing and finishing processes. Wastewater from printing and dyeing units is often rich in color. The presence of even very low concentrations of dyes in the effluent is highly visible and undesirable. The effluent also contains residues of reactive dyes and harmful chemicals. Therefore, such wastewater needs to be properly treated before its release into the environment. Among the physical, chemical, and biological decolorization technologies available, the physical sorption technique is an effective and attractive process for the treatment of dye-contaminated wastewater (Aksu, 2005).

Adsorption processes using commercial activated carbon are effective for the removal of dyes from wastewater. Thus, world consumption of activated carbon is steadily increasing because of its application in pollution control (Yuan et al., 2011). Commercial activated carbon is the preferred adsorbent for the removal of pollutants from aqueous phases. However, the use of activated carbon is limited by the high costs associated with its production, in which nonrenewable and relatively expensive raw materials, such as coal and timber, are used in many countries (Martin et al., 2003). This limitation has spurred research for inexpensive alternatives and low-cost adsorbents.

As an alternative to coal and timber, biochar is the pyrolytic product of organic waste, including municipal solid waste and agricultural waste, under partial or complete absence of oxygen. Biochars produced from different types of organic waste can absorb wastewater pollutants, such as phenol (Tan et al., 2009), dye (Yuan et al., 2011), and heavy metals (Chen et al., 2011). Thus, biochar is being considered as a waste disposal and recycling option (Gupta

---

[*] Corresponding author. Tel./fax: +86 5926190769.
E-mail address: wsluo@iue.ac.cn (W. Luo).

0960-8524/$ - see front matter © 2013 Elsevier Ltd. All rights reserved.
http://dx.doi.org/10.1016/j.biortech.2013.04.116

et al., 2009). Renewable and cheaper precursors, such as coconut husk and shell (Mohd Din et al., 2009), cattle manure (Qian et al., 2007), crop residue (Chun et al., 2004), oil palm empty fruit (Tan et al., 2009) and eucalyptus (Patnukao and Pavasant, 2008) have been used to produce biochar. Recently, using residues of anaerobic digestion to produce biochar has been investigated to expand the substrate application scopes of biochar technology. Inyang et al. (2010) prepared biochar from the digested residue of bagasse at 600 °C in nitrogen environment. Yuan et al. (2011) and Wang et al. (2011) employed biogas residue for the preparation of activated carbons by phosphoric acid (H_3PO_4) activation under nitrogen gas flow protection. Yao et al. (2011) also produced biochars from anaerobically digested sugar beet tailings through slow-pyrolysis at 600 °C. However, no study employed the palm bark and residue of anaerobic co-digested food waste and grass to produce biochar. In addition, in all previous studies, biochar production method involved high-temperature carbonization (>500 °C), chemical reagents activation (such as H_3PO_4) and nitrogen flow protection, which lead to high energy consumption.

The focus of this study was to evaluate the adsorption potential for removing cationic methylene blue dye (MB) using biochar produced from anaerobic digestion residue (BC-R), palm bark (BC-PB), and eucalyptus (BC-E). A rotary furnace set to a low temperature without nitrogen flow protection and activation was used for the experiment. The kinetic and equilibrium data of the adsorption process were used to study the adsorption mechanism of the MB molecules. This study aimed to use a new equipment to produce biochars at a relatively low temperature without nitrogen flow protection and activation treatment to save energy consumption and improve waste management strategies.

2. Methods

2.1. Materials

Biomass waste solids of eucalyptus and palm bark were collected from a garden in Xiamen, China. Residues of anaerobic digestion were obtained from a midscale anaerobic reactor for the co-digestion of food waste and Chinese silver grass. MB adsorption experiments are widely used for the evaluation of adsorbents because this dye is considered as a model for visible pollution as a result of its strong adsorption onto solids and toxicity to humans and animals. Thus, MB was selected as a model organic contaminant in this study, and the dye was purchased from Sinopharm Chemical Reagent. A stock solution of 1000 mg L^{-1} MB was prepared in a brown volumetric flask and diluted to the required concentrations (5–250 mg L^{-1}). MB and the other reagents used in this work were all analytical-grade reagents.

2.2. Biochar preparation

All organic solid wastes were sieved to less than 50 mm and then carbonized under oxygen-limited conditions in a homemade midscale low-temperature rotary furnace, which consisted of a gas source, combustion system, automatic temperature control system, mechanical mixing system, and rotary furnace body with an effective volume of 75 L. The biochar precursors were placed in the rotary carbonization chamber through the material inlet and were completely dried at 200 °C at the initial stage. Heating at 200 °C is considered torrefaction, during which the biomass is completely dried and the hemicellulose undergoes limited devolatilization and carbonization (Cao and Harris, 2010). The temperature was further raised to 400 °C at a rate of approximately 5 °C min^{-1} and was held for 30 min. The inner furnace body was rotated for an even distribution of heat and carbonization. The furnace was turned off after holding the temperature at 400 °C for 30 min, and the biochar was allowed to cool to room temperature. All biochar samples were then subjected to physical and chemical characterization to evaluate their adsorption performances.

2.3. Biochar characterization

Prior to analysis, the samples were dried overnight at 105 °C and then cooled in a desiccator. The pH values of the biochar samples were measured in deionized water at a ratio of 1:5 wt/wt (Gaskin et al., 2008). The specific surface areas and porous textures of BC-R, BC-PB, and BC-E were measured by nitrogen adsorption at 77 K using a surface area and porosimetry system (ASAP 2020M+C, USA). The biochar samples were also characterized through X-ray diffraction (XRD) and Fourier-transform infrared spectroscopy (FT-IR). X'Pert Pro (Netherlands) and Nicolet iS10 (USA) were used to investigate the crystal structure of the minerals and the presence of surface functional groups, respectively. XRD for the biochar was measured using Cu Kα radiation at 40 kV and 40 mA over the range 5° to 80° (2θ) at a scan speed of 6° min^{-1}. Infrared spectra were obtained in the range of 400–4000 cm^{-1}. The surface characteristics of the biochar were analyzed using field emission-scanning electron microscopy (FE-SEM, Hitachi S-4800, Japan). Elemental analysis was performed using a CNS and CHNS-O-Cl analyzer (Vario MAX, Germany).

2.4. Adsorption experiments

Adsorption experiments were performed to determine and compare the adsorption potential of the different biochar samples produced using the homemade low-temperature furnace. First, the effect of biochar dose on the adsorption process was investigated by adding different concentrations (2, 4, 6, and 8 g L^{-1}) of biochar to 250 mL Erlenmeyer flasks containing 200 mL of 5 mg L^{-1} MB. The samples were then placed in a shaking incubator at 180 rpm and 30 °C. A solution of 8 g L^{-1} of biochar was used to determine the effect of temperature on MB removal at 30, 40, and 50 °C, successively. Finally, to determine the effect of pH solution on the adsorption process, 8 g L^{-1} of biochar was added to Erlenmeyer flasks containing 200 mL of 5 mg L^{-1} MB, and the flasks were placed in a shaking incubator at 180 rpm and 40 °C. The solution pH values were adjusted to 5, 7, and 9 by adding NaOH (1 M) or HCl (1 M) solutions.

2.5. Adsorption kinetics

The adsorption kinetics of the biochars was determined by adding 8 g L^{-1} biochar to 200 mL of 5, 10, and 15 mg L^{-1} MB solutions. Adsorption temperature was maintained at 40 °C in a shaking incubator. At specific times, the suspensions were filtered, and equilibrium concentrations were measured at 665 nm using a UV–visible spectrophotometer (UV-5200, Shanghai). The amount of adsorbed MB at equilibrium q_e (mg g^{-1}) was calculated following Mohd Din et al. (2009):

$$q_e = V(C_0 - C_e)/w \tag{1}$$

where C_0 and C_e (mg L^{-1}) are the liquid-phase initial and equilibrium concentrations of MB, respectively. V (L) is the volume of the MB solution, and w (g) is the mass of dry biochar used.

The progress of the adsorption process was monitored by measuring the absorbance of MB in the filtered 5 mL samples. The amount of adsorbed MB at different time intervals was calculated using the following equation:

$$q_t = V(C_0 - C_t)/w \tag{2}$$

where q_t (mg g^{-1}) is the amount of MB adsorbed, and C_t (mg L^{-1}) is the concentration of the MB solution at time t.

The study of sorption kinetics provides valuable insights into the reaction pathways and into the mechanism of sorption reactions. In order to study the rate-determining step for the adsorption of MB onto the surface of biochars prepared, two kinetic models were employed: pseudo-first-order and second-order model. The linear-form equations are described following Mohd Din et al. (2009), Shawabkeh and Tutunji (2003) and Ho and McKay (1999).

The pseudo-first-order kinetic equation is:

$$\ln(q_e - q_t) = \ln q_e - k_1 t \tag{3}$$

where k_1 is the constant of a pseudo-first-order rate (min^{-1}), and q_e (mg g^{-1}) refers to the amounts of MB adsorbed at equilibrium. The values of $\ln(q_e - q_t)$ are calculated from the experimental data and plotted against t, and k_1 is calculated from the slope of the plot.

The pseudo-second-order kinetic equation is:

$$\frac{t}{q_t} = \frac{1}{k_2 q_e^2} + \frac{t}{q_e} \tag{4}$$

where k_2 (g mg^{-1} min^{-1}) is the constant of the relevant adsorption rate. The values of t/q_t are plotted against t, and the predicted adsorption capacity q_e (mg g^{-1}) and k_2 are calculated from the slope and intercept of the plot, respectively.

To further quantitatively verify the accuracy of the model, the normalized standard deviation q (%) was also calculated using the following equation:

$$\Delta q\ (\%) = 100^{*}\sqrt{\frac{\sum((q_{t,\mathrm{exp}} - q_{t,\mathrm{cal}})/q_{t,\mathrm{exp}})^2}{\mathrm{i} - 1}} \tag{5}$$

where $q_{t,\mathrm{exp}}$ and $q_{t,\mathrm{cal}}$ refer to the experimental and calculated values, and i is the number of data points.

2.6. Adsorption isotherm models

In this work, biochar (8 g L^{-1}) was blended with 10 sets of MB solution with initial concentrations that varied from 10 to 250 mg L^{-1} at a constant temperature of 40 °C in a shaking incubator at 180 rpm. All samples were equilibrated for 24 h, and the equilibrium MB concentrations were measured using a UV–visible spectrophotometer. The equilibrium data were then fitted using the Langmuir and Freundlich isotherm models.

The Langmuir isotherm model, which assumes homogeneous monolayer surface sorption, can be written as (Gupta et al., 2011; Tan et al., 2009):

$$\frac{C_e}{q_e} = \frac{1}{Q_0 K_\mathrm{L}} + \frac{C_e}{Q_0} \tag{6}$$

where Q_0 is the maximum sorption capacity of the adsorbent (mg g^{-1}), and K_L refers to the Langmuir constants related with adsorption capacity and adsorption rate. When C_e/q_e is plotted against C_e, a straight line with a slope of $1/Q_0$ and an intercept of $1/(Q_0 K_L)$ is obtained.

The Freundlich isotherm model is an empirical equation assuming heterogeneous adsorptive energies on the adsorbent surface, which can be written as (Gupta et al., 2011; Tan et al., 2009):

$$\log q_e = \log K_\mathrm{F} + \frac{1}{n}\log C_e \tag{7}$$

where K_F and n are the Freundlich constants related to adsorption capacity and intensity, respectively.

3. Results and discussion

3.1. Biochar characterization

The elemental composition and physical parameters of the biochars are presented in Table 1. Carbon was the major constituent of BC-R, BC-PB, and BC-E, which indicates that the adsorbents had a carbonaceous nature. The Brunauer–Emmett–Teller surface areas of BC-R, BC-PB, and BC-E were 7.60, 2.46, and 10.35 m^2 g^{-1}, respectively. The pore diameters were 6.70, 4.75, and 2.29 nm, indicating that the pores were mesoporous.

The XRD spectra of BC-R, BC-PB, and BC-E carbonized at 400 °C are shown in Supplementary Fig. S1a. The XRD patterns for BC-R revealed sharp peaks, which show a high degree of crystallinity with characteristic peaks at 29.4°, 36.0°, 39.4°, 43.2°, 47.5°, and 48.6°. These values match the characteristic peaks of calcite ($CaCO_3$) according to the database of the Joint Committee on Powder Diffraction Standards (reference code: 01-085-1108). The result obtained was due to the $CaCO_3$ that was added during the anaerobic digestion as a pH-buffering chemical was incorporated into the residues. Compared with those of BC-R, the XRD spectra of BC-PB and BC-E revealed no crystal substances.

The FT-IR spectra of the biochars showed functional group changes on the surfaces of the biochar samples (Supplementary Fig. S1b). The functional groups of FT-IR spectroscopic characteristic are listed in Table 2, which were determined as previously described by Shriner et al. (2003). For BC-R, the absorption peaks at 669 and 1380 cm^{-1} were assigned to the carbon–hydrogen bond (CH–) out-of-plane bending of alkenes and in-plane bending vibration of alkanes. The peaks at 1560 cm^{-1} were assigned to the C═O stretching of carboxyl anions. The peaks at 1650 cm^{-1} were assigned to the band of the out-of-plane bending of carbonates (C═O). The peaks at 1120 cm^{-1} were assigned to the C═O stretching and bending of ketones. The peaks at 1510 cm^{-1} were assigned to substituted benzene carbon skeleton vibration ($\nu_{C=C}$). The peak at 2360 cm^{-1} was attributed to the C–O vibrations in the carbon dioxide molecule (Mozia et al., 2005). The changes in the peaks and their intensities for BC-PB and BC-E were similar to those for BC-R, indicating that the functional groups on the biochars prepared from different solid waste biomass were similar. This result was caused by the strong dependence of the carbonization extent of the biomass on production temperature (Cao and Harris, 2010). The differences in the FT-IR spectra reflected water loss, organic matter degradation, and concentration of mineral components that resulted from heat-induced mass losses.

Supplementary Fig. S2a–c, d–f, and g–i show the FE-SEM micrographs of BC-R, BC-PB, and BC-E, respectively, which indicate that the clear and well-developed pore structure of the biochar consisted of cylinder-like tubes. As shown in Supplementary Fig. S2a, d, and g, all the biochar samples exhibited a rough and uneven surface texture. Supplementary Fig. S2b and c also show that BC-R contained microparticles and micropores. Similar micrographs were also observed for the inner portion of BC-PB (Supplementary Fig. S2e and f), and the walls of the cylinders were composed of layers of flat sheets. The pores mainly developed along the axis parallel to the cylindrical structure of the samples. A similar micrograph was also observed for the activated carbon prepared from oil palm empty fruit bunch by Hameed et al. (2009). Supplementary Fig. S2h and i demonstrate a homogeneous pore size distribution with a pore arrangement that was quite uniform for BC-E. The pores in the inner portion of BC-E were well pronounced and arranged in an array of honey-combed structures. All of the FE-SEM micrographs indicate an excellent possibility for the dyes to be trapped and adsorbed by the biochars.

Table 1
Elemental composition and physical parameters of the biochars.

Biochar	Particle size (mm)	Elemental composition (%)	Proximate analysis (%)	BET surface area (m^2/g)	Micropore volume (cm^3/g)	Average pore width (nm)
BC-R	0.25–0.83	C: 63.50, H: 5.28, O:18.10, N: 0.94, S: 0.065	Moisture: 2.9, pH: 8.83	7.60	0.013	6.70
BC-PB	0.25–0.83	C: 68.90, H: 5.38, O: 20.80, N: 0.88, S: 1.52	Moisture: 4.2, pH: 7.10	2.46	0.0029	4.75
BC-E	0.25–0.83	C: 77.80, H: 5.38, O: 18.30, N: 0.41, S: 0.056	Moisture: 4.1, pH: 7.47	10.35	0.0059	2.29

Table 2
FT-IR spectral characteristics of BC-R, BC-PB and BC-E.

IR peak	Frequency (cm^{-1})	Assignment
1	669	CH– of alkenes and alkanes
2	1120	C=O stretching and bending of ketones
3	1380	CH– of alkenes and alkanes
4	1510	Substituted benzene carbon skeleton vibration
5	1560	C=O stretching of carboxyl anions
6	1650	Out-of-plane bending of carbonates
7	2360	C–O vibrations of CO_2 molecule

3.2. Adsorption kinetics

3.2.1. Effect of adsorbent dose

The removal efficiencies of MB with an initial concentration of 5 mg L^{-1} at 30 °C by BC-R, BC-PB, and BC-E are shown in Fig. 1. The efficiency of MB removal increased with increasing biochar dose at a constant MB concentration. For BC-R, the removal efficiency increased from 51.9% to 96.4% with the increase in biochar dose from 2 to 8 g L^{-1} within the equilibration time of 120 min (Fig. 1a). For BC-PB (Fig. 1b) and BC-E (Fig. 1c), a similar trend was observed for the removal efficiency from aqueous solution, and the removal efficiency increased from 38.5% to 89.8% for BC-PB and 25.1% to 78.3% for BC-E. The appropriate biochar dose was found to be 8 g L^{-1}. The increase in removal efficiency can be attributed to the increase in available sorption surface and the availability of more adsorption sites. A similar behavior was reported for the adsorption of MB on papaya seeds (Hameed, 2009). The efficiency of MB removal was lower for BC-E than for BC-R and BC-PB, which may be attributed to the influence of the pore size of BC-E and the molecular dimension of MB. The average pore width of 2.29 nm for BC-E is close to the molecular dimensions of MB (width, 1.43 nm; depth, 0.61 nm; thickness, 0.40 nm), which can hinder the adsorption of MB from solution (Pelekani and Snoeyink, 2000).

3.2.2. Effect of temperature

Effect of temperature on adsorption capacity for MB onto biochar was investigated at temperatures of 30, 40 and 50 °C, respectively. As shown in Fig. 2a–c, the effect of temperature on adsorption performance for MB onto biochars was different at different temperatures. For BC-R, the effect of temperature on the adsorption performance of MB is not obvious as shown in Fig. 2a. Thus, it is not a valid conclusion that the adsorption performance of MB on BC-R can be enhanced by increasing of the temperature. For BC-E, the temperature has slight effect on the adsorption performance as temperature increased from 30 to 40 °C as shown in Fig. 2c. As temperature further increased to 50 °C, the effect of temperature on the adsorption performance is negligible for BC-E. Compared with BC-R and BC-E, Fig. 2b demonstrated that the adsorption performance of MB was significantly enhanced with the increase in temperature up to 50 °C, which indicates that higher temperatures may exhibit a positive impact on MB removal by adsorption onto BC-PB. Similar observations were also reported in the literatures. Bulut and Aydin (2006) reported that the removal of MB by adsorption onto wheat shells increased from 16.56 to 21.50 mg g^{-1} by increasing the temperature of the solution from 303 to 323 K. Hameed and Ahmad (2009) observed that the adsorption capacity of MB increased from 82.64 to 142.86 mg g^{-1} when the temperature of the solution was increased from 303 to 323 K. This result probably occurred because of the increase in diffusion rate of MB with increasing temperature. An increased number of MB molecules may also acquire sufficient energy to interact with active sites at the biochar surface (2009b). This result may also be attributed to the increase in the porosity and total pore volume of the adsorbent and even to the increase in the number of available active surface sites for adsorption (Aksu et al., 2008).

3.2.3. Effect of solution pH

The effect of solution pH on MB removal is shown in Fig. 3. The pH did not show any significant effect on the efficiency of MB removal by BC-R and BC-PB. With the solution pH varying from 5.0 to 9.0 for 120 min, the efficiencies of MB removal were between 99.4% and 99.9% for BC-R (Fig. 3a) and 99.3% and 99.7% for BC-PB (Fig. 3b). For BC-R (Fig. 3c), the removal efficiency decreased slightly in the pH range 5–9. The efficiency of MB removal usually increases as the pH is increased (Kavitha and Namasivayam, 2007).

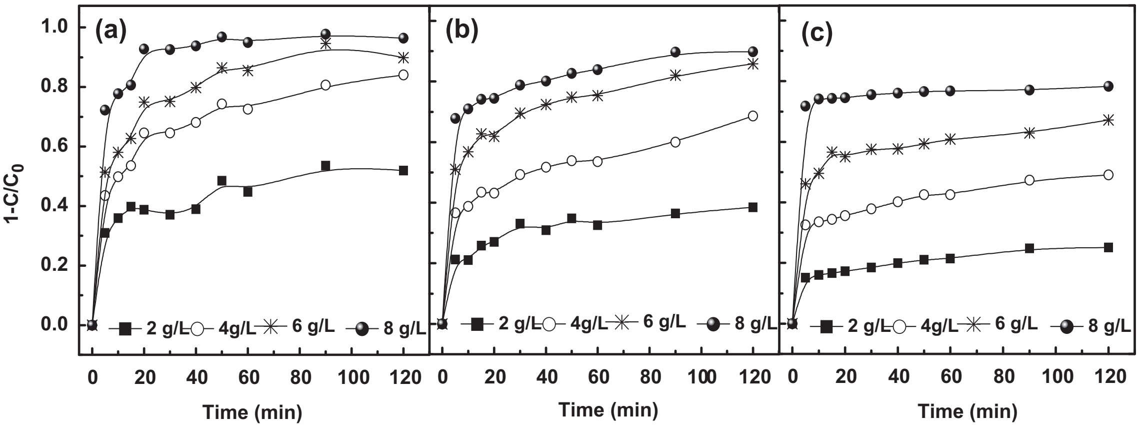

Fig. 1. Effect of biochar dose on the removal efficiency of MB: (a) BC-R, (b) BC-PB, and (c) BC-E.

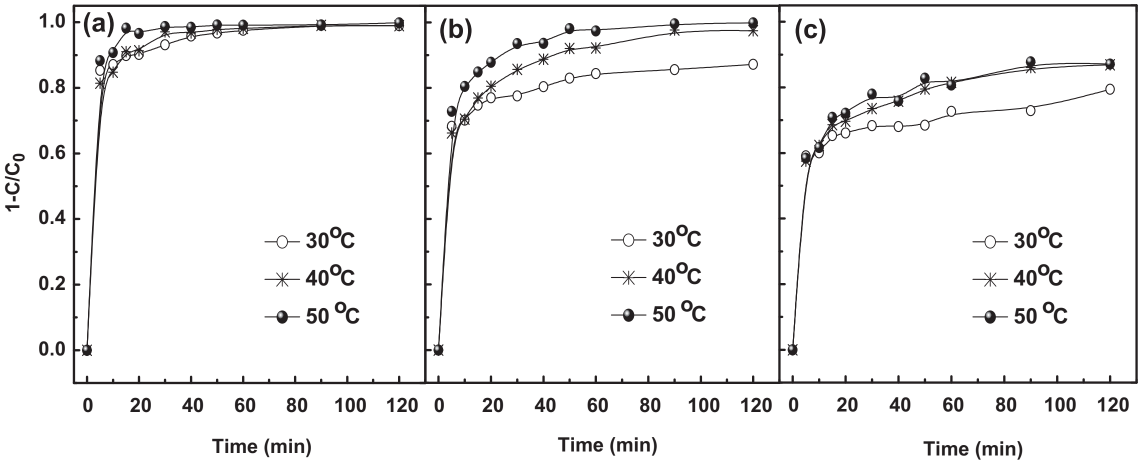

Fig. 2. Effect of temperature on the removal efficiency of MB: (a) BC-R, (b) BC-PB, and (c) BC-E.

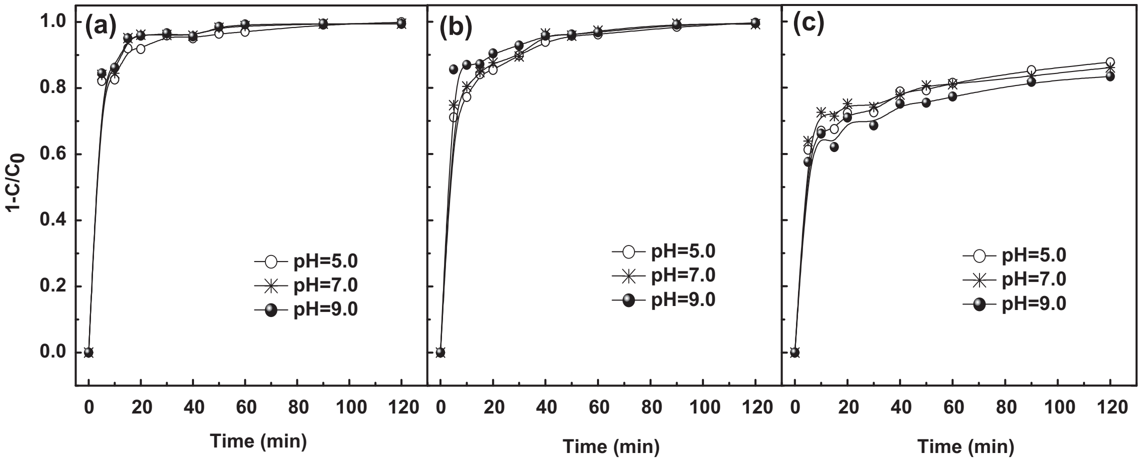

Fig. 3. Effect of pH on the removal efficiency of MB: (a) BC-R, (b) BC-PB, and (c) BC-E.

This minor variation can be explained by the nature of BC-E at different pH values in MB adsorption. The cell wall of BC-E contains many surface functional groups. Some functional groups carrying a positive charge would be exposed because of the hydrolysis of BC-E at higher pH, which inhibits the adsorption of positively charged MB cations through electrostatic forces of attraction. Therefore, electrostatic adsorption is not the only mechanism of adsorption for MB. Similar descriptions have been reported on the sorption of basic red 18 on activated clay (Ho et al., 2001) and MB adsorption on papaya seeds (Hameed, 2009) and neem leaf powder (Bhattacharyya and Sharma, 2005).

3.3. Adsorption kinetics

MB adsorption as a function of time and concentration was fitted with the pseudo-first-order, pseudo-second-order kinetic models and shown in Fig. 4 while the parameters of kinetics are shown in Table 3. The adsorption of MB increased from 0.626 to 1.714 mg g^{-1}, 0.633–1.173 mg g^{-1} and 0.593–0.935 mg g^{-1} as the concentrations of MB increased from 5 to 15 mg L^{-1} for BC-R, BC-PB and BC-E, respectively. When comparing with previous studies, the adsorption capacity of biochars prepared was lower than the commercial activated carbon (paticle size: 90 μm) 149.25–296.45 mg g^{-1} reported by Kannan and Sundaram (2001), probably because of the differences in original materials, particle size of biochars, and the preparation conditions of short carbonization time and low carbonization temperature without any activation and nitrogen flow protection in the present study. However, the adsorption capacity of biochar prepared in this study were better than those activated carbon prepared from fir wood, almond shell and walnut shell, etc. (Rafatullah et al., 2010). In addition, both models fit the results based on the correlation coefficient R^2 and the actual test results. R^2 for the pseudo-second-order kinetics were higher than the R^2 for the pseudo-first-order kinetic, and the calculated q_e results were in agreement with the experimental q_e values. These results indicate that the adsorption kinetics is better represented by the pseudo-second-order kinetic model. Similarly, the experimental adsorption capacity values were closer to the calculated adsorption capacity values for the pseudo-second-order kinetic model than those for the pseudo-first-order model. While the assumption of the pseudo-first-order model was physical adsorption and the solute uptake rate with time is directly proportional to ratio of the solute concentration and the amount of solid (Shawabkeh and Tutunji, 2003), the pseudo-second-order kinetic model is based on the assumption that the rate-limiting step may be chemical sorption or chemisorption involving valence forces through sharing or exchange of electrons between sorbent and sorbate (Ho and McKay, 1999). Therefore, it is likely that MB adsorbed on biochar involving chemical reactions.

The normalized standard deviation Δq for the pseudo-first-order kinetics was between 10.92% and 23.29% for BC-R, 7.88% and 16.98% for BC-PB, and 11.92% and 17.41% for BC-E, which are higher than those for the pseudo-second-order kinetic equation. The pseudo-second-order kinetic model indicated the lowest Δq

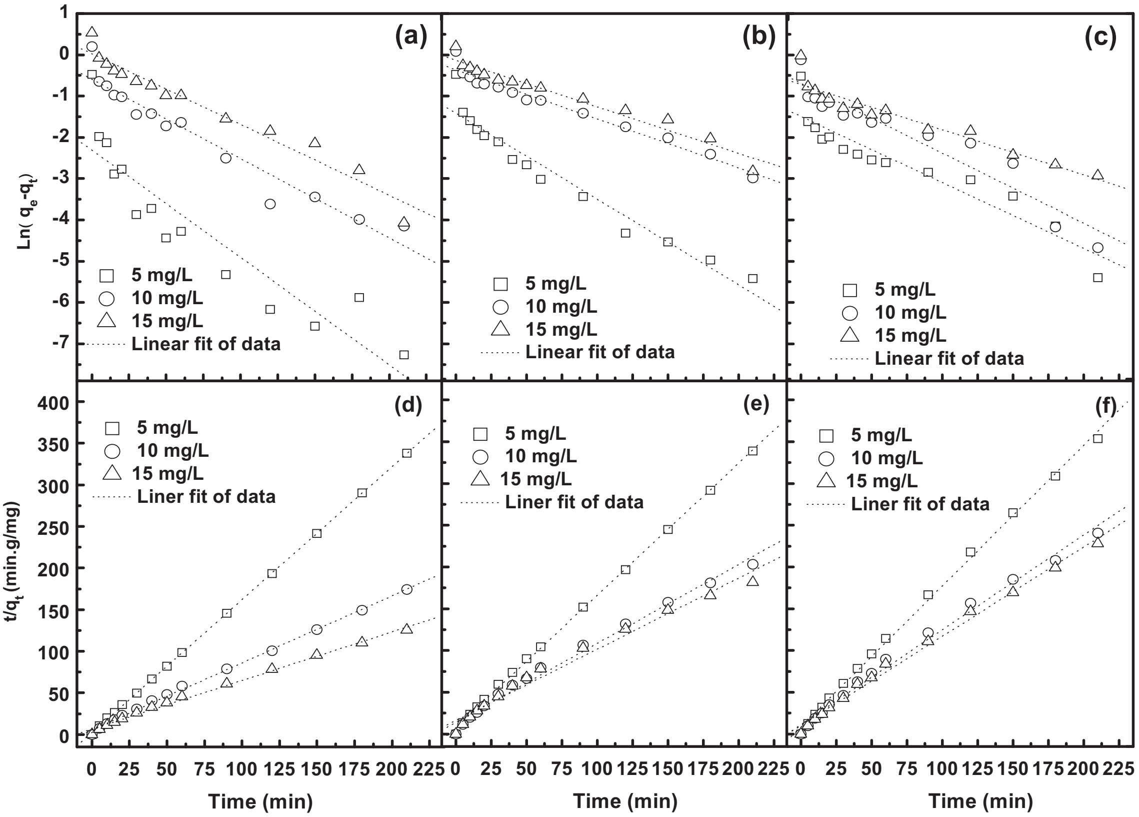

Fig. 4. Pseudo-first-order kinetics for the adsorption of MB on (a) BC-R, (b) BC-PB, and (c) BC-E; pseudo-second-order kinetics for the adsorption of MB on (d) BC-R, (e) BC-PB, and (f) BC-E.

Table 3
Kinetic parameters of the pseudo-first and pseudo-second order kinetic models for MB adsorption at 40 °C.

MB concentration (mg L^{-1})	$q_{e,exp}$ (mg g^{-1})	Pseudo-first order parameters				Pseudo-second order parameters			
		k_1 (min^{-1})	$q_{e,cal}$ (mg g^{-1})	R^2	Δq (%)	k_2 (g mg^{-1} min^{-1})	$q_{e,cal}$ (mg g^{-1})	R^2	Δq (%)
BC-R									
5	0.622	0.026	0.0997	0.8401	23.29	1.072	0.626	0.9999	0.18
10	1.222	0.0192	0.553	0.9373	15.18	0.115	1.242	0.9981	0.45
15	1.694	0.0172	1.027	0.9544	10.92	0.0530	1.714	0.995	0.33
BC-PB									
5	0.624	0.0208	0.242	0.9457	16.98	0.307	0.633	0.9993	0.40
10	1.085	0.0119	0.692	0.9658	10.04	0.0636	1.058	0.9888	0.69
15	1.217	0.0112	0.871	0.9538	7.88	0.0446	1.173	0.9788	1.00
BC-E									
5	0.599	0.016	0.223	0.8834	17.41	0.331	0.593	0.9981	0.28
10	0.882	0.017	0.503	0.9104	11.92	0.113	0.881	0.9916	0.031
15	0.957	0.0109	0.485	0.9144	13.68	0.113	0.935	0.9939	0.64

values, which ranged from 0.18% to 0.45%, 0.40% to 1.00%, and 0.031% to 0.64% for BC-R, BC-PB, and BC-E, respectively. Based on the highest R^2 values and the lowest Δq values that approached unity, the pseudo-second-order model was the most suitable equation to describe the adsorption kinetics of MB on the biochars. The findings were similar to the previous works on the adsorption of MB onto sugarcane bagasse (Yu et al., 2012) and oil palm shell (Foo and Hameed, 2013) based-activated carbons.

3.4. Adsorption isotherms

The sorption equilibrium data were analyzed using the Langmuir and Freundlich isotherm models (Fig. 5a and b). The isotherm parameters calculated from the models together with R^2 are listed in Table 4. The highest R^2 values corresponded to the Langmuir model with the R^2 values 0.969, 0.986, and 0.990 for BC-R, BC-PB, and BC-E, respectively. The correlation found using the Freundlich isotherm model was lower that using the Langmuir isotherm model, with the R^2 values 0.911, 0.906, and 0.889 for BC-R, BC-PB, and BC-E, respectively. Meanwhile, the value of the exponent n was greater than 1, which represents a favorable adsorption condition. The perfect fit of the experimental data with the Langmuir isotherm model indicates that the adsorption behavior observed was predominantly monolayer adsorption, which involves chemical and physical adsorption. This observation is in agreement with previous reports on MB adsorption onto activated carbon prepared from hazelnut husks (Ozer et al., 2012) and rattan sawdust (Hameed et al., 2007).

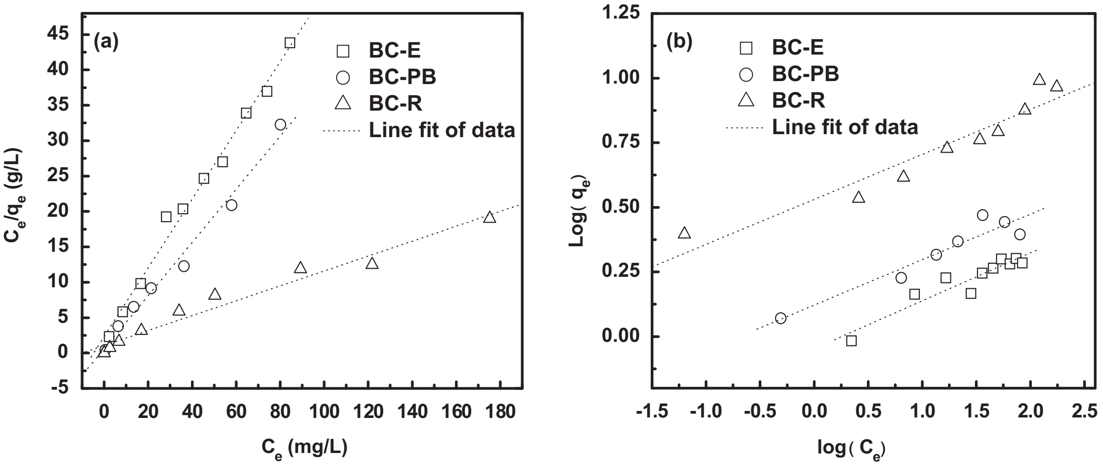

Fig. 5. Adsorption isotherms of MB on biochars: (a) Langmuir and (b) Freundlich.

Table 4
Langmuir and Freundlich isotherm constants for the adsorption of MB onto the biochars.

Biochar	Langmuir constants				Freundlich constants		
	$Q_{0,cal}$ (mg g^{-1})	$Q_{0,exp}$ (mg g^{-1})	K_L	R^2	K_F (mg g^{-1})	n	R^2
BC-R	9.50	9.77	0.099	0.969	3.39	5.74	0.911
BC-PB	2.66	2.95	0.63	0.986	1.32	5.68	0.906
BC-E	2.06	2.00	0.21	0.990	0.34	5.39	0.889

4. Conclusions

Anaerobic digestion residue, palm bark, and eucalyptus were used as raw materials for the production of biochar using a home-made midscale rotary carbonization furnace. Temperature had a significant effect on MB removal by biochar and the order of the MB removal efficiency under the same conditions is: BC-R > BC-PB > BC-E. The pseudo-second-order kinetic model most suitably described the adsorption of MB onto the three types of biochars. Compared with the Freundlich isotherm model, the Langmuir isotherm model was more suitable for describing the adsorption of MB on biochars. BC-R achieved a maximum sorption capacity of 9.50 mg g^{-1}.

Acknowledgement

This work was financially supported by grants from the Xiamen Science Foundation (3502Z20111049), Fujian Science Funding (2012Y0067), China Postdoctoral Science Foundation (2013M530747), and Natural Science Foundation of China (51208492).

Appendix A. Supplementary data

Supplementary data associated with this article can be found, in the online version, at http://dx.doi.org/10.1016/j.biortech.2013.04.116.

References

Aksu, Z., 2005. Application of biosorption for the removal of organic pollutants: a review. Process Biochem. 40, 997–1026.

Aksu, Z., Tatlı, A.İ., Tunç, Ö., 2008. A comparative adsorption/biosorption study of Acid Blue 161: effect of temperature on equilibrium and kinetic parameters. Chem. Eng. J. 142, 23–39.

Bhattacharyya, K.G., Sharma, A., 2005. Kinetics and thermodynamics of methylene blue adsorption on neem (*Azadirachta indica*) leaf powder. Dyes Pigm. 65, 51–59.

Bulut, Y., Aydın, H., 2006. A kinetics and thermodynamics study of methylene blue adsorption on wheat shells. Desalination 194, 259–267.

Cao, X., Harris, W., 2010. Properties of dairy-manure-derived biochar pertinent to its potential use in remediation. Bioresour. Technol. 101, 5222–5228.

Chen, X., Chen, G., Chen, L., Chen, Y., Lehmann, J., McBride, M.B., Hay, A.G., 2011. Adsorption of copper and zinc by biochars produced from pyrolysis of hardwood and corn straw in aqueous solution. Bioresour. Technol. 102, 8877–8884.

Chun, Y., Sheng, G., Chiou, C.T., Xing, B., 2004. Compositions and sorptive properties of crop residue-derived chars. Environ. Sci. Technol. 38, 4649–4655.

Foo, K.Y., Hameed, B.H., 2013. Utilization of oil palm biodiesel solid residue as renewable sources for preparation of granular activated carbon by microwave induced KOH activation. Bioresour. Technol. 130, 696–702.

Gaskin, J.W., Steiner, C., Harris, K., Das, K.C., Bibens, B., 2008. Effect of low-temperature pyrolysis conditions on biochar for agricultural use. Trans. ASABE 51, 2061–2069.

Gupta, V.K., Carrott, P.J.M., Ribeiro Carrott, M.M.L., Suhas, 2009. Low-cost adsorbents: growing approach to wastewater treatment – a review. Crit. Rev. Environ. Sci. Technol. 39, 783–842.

Gupta, V.K., Gupta, B., Rastogi, A., Agarwal, S., Nayak, A., 2011. A comparative investigation on adsorption performances of mesoporous activated carbon prepared from waste rubber tire and activated carbon for a hazardous azo dye-Acid Blue 113. J. Hazard. Mater. 186, 891–901.

Hameed, B.H., 2009. Evaluation of papaya seeds as a novel non-conventional low-cost adsorbent for removal of methylene blue. J. Hazard. Mater. 162, 939–944.

Hameed, B.H., Ahmad, A.A., 2009. Batch adsorption of methylene blue from aqueous solution by garlic peel, an agricultural waste biomass. J. Hazard. Mater. 164, 870–875.

Hameed, B.H., Ahmad, A.L., Latiff, K.N.A., 2007. Adsorption of basic dye (methylene blue) onto activated carbon prepared from rattan sawdust. Dyes Pigm. 75, 143–149.

Hameed, B.H., Tan, I.A.W., Ahmad, A.L., 2009. Preparation of oil palm empty fruit bunch-based activated carbon for removal of 2,4,6-trichlorophenol: optimization using response surface methodology. J. Hazard. Mater. 164, 1316–1324.

Ho, Y.S., Chiang, C.C., Hsu, Y.C., 2001. Sorption kinetics for dye removal from aqueous solution using activated clay. Sep. Sci. Technol. 36, 2473–2488.

Ho, Y.S., McKay, G., 1999. Pseudo-second order model for sorption processes. Process Biochem. 34, 451–465.

Inyang, M., Gao, B., Pullammanappallil, P., Ding, W., Zimmerman, A.R., 2010. Biochar from anaerobically digested sugarcane bagasse. Bioresour. Technol. 101, 8868–8872.

Kannan, N., Sundaram, M.M., 2001. Kinetics and mechanism of removal of methylene blue by adsorption on various carbons-a comparative study. Dyes Pigm. 51, 25–40.

Kavitha, D., Namasivayam, C., 2007. Experimental and kinetic studies on methylene blue adsorption by coir pith carbon. Bioresour. Technol. 98, 14–21.

Martin, M.J., Artola, A., Balaguer, M.D., Rigola, M., 2003. Activated carbons developed from surplus sewage sludge for the removal of dyes from dilute aqueous solutions. Chem. Eng. J. 94, 231–239.

Mohd Din, A.T., Hameed, B.H., Ahmad, A.L., 2009. Batch adsorption of phenol onto physiochemical-activated coconut shell. J. Hazard. Mater. 161, 1522–1529.

Mozia, S., Tomaszewska, M., Morawski, A.W., 2005. Studies on the effect of humic acids and phenol on adsorption–ultrafiltration process performance. Water Res. 39, 501–509.

Ozer, C., Imamoglu, M., Turhan, Y., Boysan, F., 2012. Removal of methylene blue from aqueous solutions using phosphoric acid activated carbon produced from hazelnut husks. Toxicol. Environ. Chem. 94, 1283–1293.

Patnukao, P., Pavasant, P., 2008. Activated carbon from *Eucalyptus camaldulensis Dehn* bark using phosphoric acid activation. Bioresour. Technol. 99, 8540–8543.

Pelekani, C., Snoeyink, V.L., 2000. Competitive adsorption between atrazine and methylene blue on activated carbon: the importance of pore size distribution. Carbon 38, 1423–1436.

Qian, Q., Machida, M., Tatsumoto, H., 2007. Preparation of activated carbons from cattle-manure compost by zinc chloride activation. Bioresour. Technol. 98, 353–360.

Rafatullah, M., Sulaiman, O., Hashim, R., Ahmad, A., 2010. Adsorption of methylene blue on low-cost adsorbents: a review. J. Hazard. Mater. 177, 70–80.

Shawabkeh, R.A., Tutunji, M.F., 2003. Experimental study and modeling of basic dye sorption by diatomaceous clay. Appl. Clay Sci. 24, 111–120.

Shriner, R.L., Fuson, R.C., Curtin, D.Y., Fuson, R.F., 2003. The Systematic Identification of Organic Compounds, eighth ed. John Wiley & Sons, New York.

Tan, I.A.W., Ahmad, A.L., Hameed, B.H., 2009. Adsorption isotherms, kinetics, thermodynamics and desorption studies of 2,4,6-trichlorophenol on oil palm empty fruit bunch-based activated carbon. J. Hazard. Mater. 164, 473–482.

Wang, Z., Nie, E., Li, J., Zhao, Y., Luo, X., Zheng, Z., 2011. Carbons prepared from *Spartina alterniflora* and its anaerobically digested residue by H_3PO_4 activation: characterization and adsorption of cadmium from aqueous solutions. J. Hazard. Mater. 188, 29–36.

Yao, Y., Gao, B., Inyang, M., Zimmerman, A.R., Cao, X., Pullammanappallil, P., Yang, L., 2011. Biochar derived from anaerobically digested sugar beet tailings: characterization and phosphate removal potential. Bioresour. Technol. 102, 6273–6278.

Yu, J.X., Chi, R.A., Zhang, Y.F., Xu, Z.G., Xiao, C.Q., Guo, J., 2012. A situ co-precipitation method to prepare magnetic PMDA modified sugarcane bagasse and its application for competitive adsorption of methylene blue and basic magenta. Bioresour. Technol. 110, 160–166.

Yuan, X.Z., Shi, X.S., Zeng, S.J., Wei, Y.L., 2011. Activated carbons prepared from biogas residue: characterization and methylene blue adsorption capacity. J. Chem. Technol. Biotechnol. 86, 361–366.